Available online at www.sciencedirect.com
SCIENCE DIRECT®
Journal of Nuclear Materials 329–333 (2004) 1199–1203
journal of nuclear materials
www.elsevier.com/locate/jnucmat

The effects of grain boundary structure on binding of He in Fe

R.J. Kurtz *, H.L. Heinisch

Pacific Northwest National Laboratory, P.O. Box 999, Richland, WA 99352, USA

Abstract

Computer simulations were performed to explore the effect of grain boundary (GB) structure and properties on the binding of He to boundaries in Fe. Symmetrical tilt GBs spanning a range of GB energies and excess volumes were examined. Molecular statics was used to map the He trapping efficiency at numerous substitutional and interstitial sites in and near each GB. The results showed that both substitutional and interstitial He atoms were trapped at GBs. Interstitial He was more strongly bound ($E^i_{gb} \sim 0.5$–2.7 eV) to the GB core than substitutional He ($E^s_{gb} \sim 0.2$–0.8 eV). The He binding energy was found to increase linearly with GB excess volume. The He capture radius varied from ~0.3 to 0.7 nm and also depended on GB properties. Finally, the He binding energy varied significantly within the GB core and approximately corresponded to the variation in atomic excess volume normal to the GB plane.

1. Introduction

It is well known that fusion reactions produce high energy neutrons that interact strongly with the structural material of a fusion device. The bombarding neutrons ($E > 1$ MeV) cause nuclear transmutation reactions that produce considerable concentrations of foreign elements within the material. In particular, the He that is produced by (n, α) reactions plays an important role in the behavior of metals and alloys under irradiation since it can drastically alter mechanical properties, potentially embrittling the material even at low concentrations [1].

The solubility of He in metals is extremely low and ultimately is the reason for its detrimental effects on mechanical properties [1]. This low solubility is equivalent to a very strong tendency for He to precipitate into clusters or bubbles. Accumulation of He can have major consequences for the structural integrity of first-wall materials. At high temperatures He can result in significant degradation of the tensile, creep and fatigue properties. These effects are caused by He bubbles in the GBs that lead to initiation of cracks and premature failure under stress [2,3]. The extent of the degradation depends on the temperature, He content and production rate, stress, composition and microstructure of the material. At low temperatures He may also influence irradiation hardening [4] and fatigue life by acting as an obstacle to the movement of dislocations [5,6]. He also affects the incubation time for onset of swelling due to large increases in the cavity density [7].

Several theoretical studies have been performed yielding important understanding of He embrittlement in metals [5,8–20]. Atomistic calculations have shown that in pure nickel two He atoms are bound to each other by a few tenths of an electron volt. Each subsequent He atom is bound by a greater amount to the cluster, saturating at a binding energy of about 2 eV [5,8]. Atomistic calculations also demonstrate strong binding of He to GBs [9–11]. Helium atoms placed in a symmetric tilt boundary in nickel caused the boundary to reconstruct with the He atoms more strongly bound to each other than in the bulk [9]. Helium greatly decreased the stress at which cracks propagate. He-vacancy clusters lowered the fracture stress by an order of magnitude in nickel [12]. Helium also interacts with dislocations. For example, in nickel He is bound to dislocation cores by 0.3 eV, an energy consistent with its elastic attraction [13]. Even stronger binding to dislocations has been found in bcc metals such as molybdenum with

* Corresponding author. Tel.: +1-509 373 7515; fax: +1-509 376 0418.
E-mail address: rj.kurtz@pnl.gov (R.J. Kurtz).

0022-3115/$ - see front matter © 2004 Elsevier B.V. All rights reserved.
doi:10.1016/j.jnucmat.2004.04.262

interaction energies of about 2.1 eV [14,15]. These results suggest that at low stress levels He atoms may pin dislocations in bcc metals, while at higher stresses He may reduce the velocity of dislocations.

Atomistic calculations have successfully shed light on some of the basic interactions of He with defects in fcc metals, but very little work has been performed on bcc metals and no work has been done on alloys. While He is an interstitial impurity in both bcc and fcc lattices, its ability to be trapped appears to be different in the two structures [16]. We have initiated a systematic study to characterize the interaction of He with the damage microstructure produced during neutron irradiation of a fusion relevant structural material such as ferritic steel.

2. Grain boundary structure

2.1. Interatomic potentials and simulation methods

The Fe–He interatomic potential used in this research has been described in detail previously [21]. The potential uses the Finnis–Sinclair formalism. For the Fe–Fe component of the potential the pair interaction and electron densities were cut off at 0.37264 nm. With this cut off the cohesive energy for bcc Fe is −4.316 eV/atom and the lattice parameter is 0.28665 nm. For He–He interactions the cut off distance was decreased from the original [21] to 0.54857 nm to improve computational efficiency. The refit He–He interaction was smoothed so that the value of the potential and its first derivative at the new cut off were zero. With this change the cohesive energy of fcc He is −0.005678 eV/atom. The Fe–He interaction is cut off at 0.3800 nm. The formation energies of an interstitial He atom, a substitutional He atom, a vacancy and a self-interstitial atom were calculated to be 5.25, 3.25, 1.70 and 4.88 eV, as reported previously [21].

Most of the details pertaining to the methodology used in the calculations of the atomic arrangements of GBs have been described in detail elsewhere [22,23]. The model consists of a two part computational cell, rectangular in shape. One part, Region I contains movable atoms embedded in a semi-rigid part, Region II. The GB approximately bisects the model as shown in Fig. 1. Equilibrium, ~0 K, structures are obtained via relaxation using molecular dynamics with an energy quench. The two grains are free to move and undergo homogenous displacement in all three directions and this movement occurs during the relaxation via a viscous drag algorithm. Periodic border conditions are employed in the x and z directions.

Four symmetric tilt GBs were studied in this work, all with a common $\langle 1\,0\,1\rangle$ tilt axis. The four GBs were $\Sigma 3$ $\{1\,1\,2\}$ $\Theta = 70.53°$, $\Sigma 11$ $\{3\,2\,3\}$ $\Theta = 50.48°$, $\Sigma 9$ $\{1\,1\,4\}$ $\Theta = 38.94°$, and $\Sigma 3$ $\{1\,1\,1\}$ $\Theta = 70.53°$.

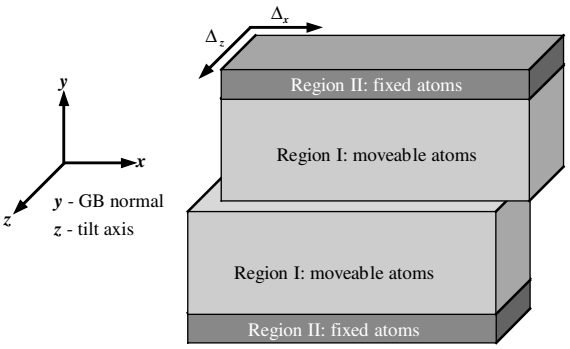

Fig. 1. Model geometry used in GB simulations. Models are periodic in the x and z directions. Δ_x and Δ_z are translation vectors parallel to the grain boundary plane.

2.2. Gamma surfaces of grain boundaries

We determined the γ-surfaces for each of the GBs by constructing a series of atomic configurations in which the grains were translated relative to one another. The cell of non-identical displacements defines the set of unique in-plane translations that can be explored [24]. This cell was divided into a grid of points. The displacement-shift-complete (DSC) lattice was used as the basis of the grid since the density of the DSC lattice is related to the size of the cell of non-identical displacements for tilt boundaries [25]. At each point on the grid a partially relaxed, ~0 K, GB energy is calculated. This partial relaxation includes local atomic displacements and rigid translations of the grains normal to the GB plane, but not parallel to it. Local minima on the γ-surface correspond to relative translations of the grains producing stable or metastable GB structures. Such structures were individually examined by full relaxation, which includes local displacements of all Region I atoms combined with simultaneous rigid-body translations of each grain both perpendicular and parallel to the GB plane. The deepest energy minimum corresponds to the ground state structure of the GB.

2.3. GB atomic structure, energy and excess volume

The calculated ground state structures for the GBs considered in this study are shown in Fig. 2. Dark and light circles denote atom positions in alternating $\{1\,0\,1\}$ planes perpendicular to the $\langle 1\,0\,1\rangle$ tilt axis. The upper and lower grains are not distinguished by different symbols. An energy distribution function was generated for each boundary by dividing the GB into a large number of slices and computing the excess potential energy E_{xs}/A for each slice, which is

$$\frac{E_{xs}}{A} = \frac{\Sigma(E_{gb} - E_p)}{L_z w}, \tag{1}$$

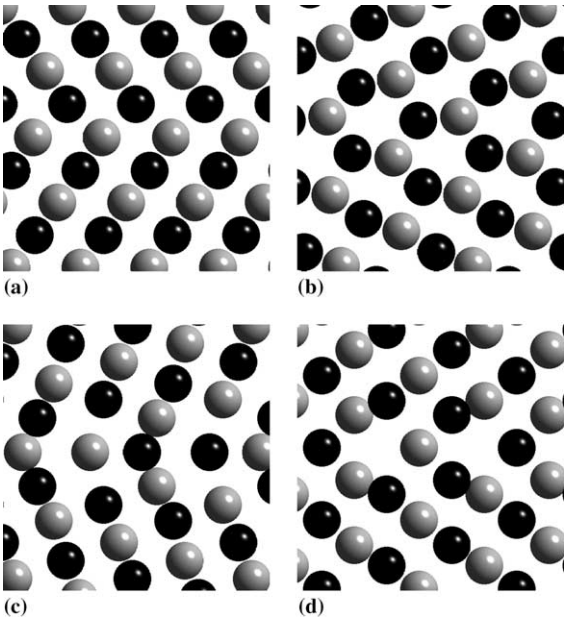

Fig. 2. Relaxed ground state atomic structures for GBs in Fe (a) $\Sigma 3$ $\{1\,1\,2\}$, (b) $\Sigma 11$ $\{3\,2\,3\}$, (c) $\Sigma 9$ $\{1\,1\,4\}$, and (d) $\Sigma 3$ $\{1\,1\,1\}$. Dark and light circles denote atom positions in alternating $\{1\,0\,1\}$ planes perpendicular to the $\langle 1\,0\,1\rangle$ tilt axis.

where E_{gb} is the potential energy of an atom in the GB model, E_p is the potential energy of an atom in a perfect crystal, L_z is the thickness of the model parallel to the tilt axis and w is the slice width. The summation is performed over all atoms in a slice. The GB energy per unit area, γ_{gb}, can be determined by integrating the energy distribution function over several repeat periods. Table 1 lists γ_{gb} for the four boundaries examined here. The GB energies are generally quite large relative to free surface energies. For the Fe potential employed here the free surface energies γ_{100}, γ_{110} and γ_{111} are 1.81, 1.58 and 2.00 J/m^2, respectively. It should be noted that the calculated free surface energies are slightly low relative to experimentally measured values for Fe, which are typically in the neighborhood of 1.6–2.3 J/m^2.

Another important property is the volume expansion normal to the GB plane. This quantity is determined by calculating the excess volume per unit area of GB. Excess atomic volumes were determined from the relation

$$\Omega_{xs} = \Omega_v - \Omega_p, \tag{2}$$

where Ω_v is the Voronoi volume of an atom in the GB model and Ω_p is the atomic volume of an Fe atom in a perfect, unstrained lattice. The Voronoi volume is the volume of a polyhedron whose faces are perpendicular bisectors of the lines connecting an atom to its nearest neighbors. The atomic volume for Fe in this study is 0.01178 nm^3. The excess volume, V_{gb}, in a rectangular patch of GB of area, A, is computed from

$$\frac{V_{gb}}{A} = \frac{\sum \Omega_{xs}}{L_x L_z}, \tag{3}$$

where L_x is the length of the GB perpendicular to the tilt axis. It is evident from the GB structures in Fig. 2 that Ω_{xs} varies considerably in directions both parallel and perpendicular to the GB plane. In order to properly compute V_{gb}/A a sufficiently large volume of material must be chosen to account for these variations. In this work we computed values of Ω_{xs} for atom planes parallel to the GB until it was essentially zero. Furthermore, values of L_x and L_z were selected to include several repeat periods in those directions so that an accurate estimate of the GB excess volume could be obtained. Table 1 gives V_{gb}/A for the GBs investigated in this study. Note there is good correlation between the GB energy and excess volume.

Table 1
Grain boundary energy and excess volume for the four symmetric tilt boundaries considered in this study

Σ	GB plane	γ_{gb} (J/m^2)	V_{gb}/A (nm)
3	$\{1\,1\,2\}$	0.30	0.007
11	$\{3\,2\,3\}$	1.00	0.022
9	$\{1\,1\,4\}$	1.40	0.036
3	$\{1\,1\,1\}$	1.51	0.041

The tilt axis is $\langle 1\,0\,1\rangle$.

3. He in grain boundaries

Binding of He to GBs was explored by insertion of a single He atom in either a substitutional (replacement of an Fe atom with He) or interstitial location, and then relaxing the simulation block. Both atomic displacements of Region I atoms and rigid-body translations of the two grains were allowed during the relaxation. Since the excess volume varies significantly in the GB core a large number of different starting positions for the He atom were examined. Binding energies at a particular site α (either substitutional or interstitial) in and near the GB core were determined from the equation

$$E_B^\alpha = E_{gb}^\alpha - E_{gb} - E_f^\alpha, \tag{4}$$

where E_{gb}^α is the energy of the GB with a He atom at site α, E_{gb} is the energy of the GB without a He atom, and E_f^α is the formation energy of a He atom at site α in bulk Fe. In Fig. 3 the substitutional or interstitial He binding energy is plotted as a function of distance from the $\Sigma 3$ $\{1\,1\,1\}$ GB. Also shown in Fig. 3 is the distance dependence of the excess volume normal to the GB plane. Three observations may be made from this plot. First, the binding energy of substitutional He is considerably

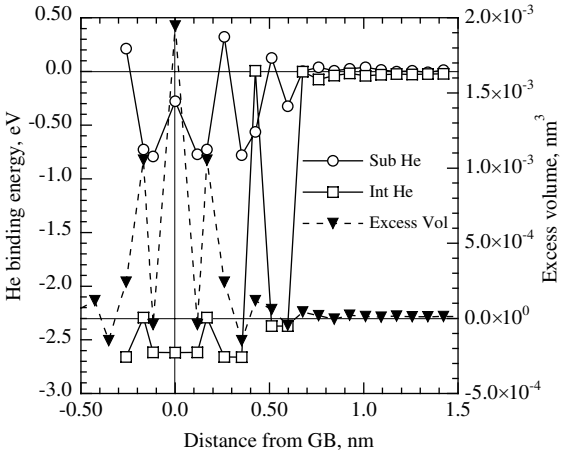

Fig. 3. Dependence of excess volume and He binding energy on distance from the GB plane.

smaller than interstitial He, indicating that interstitial He will be strongly trapped by vacancies in the GB. Relative to the bulk, interstitial He is very strongly bound to the GB, a result similar to the findings of Baskes and Vitek in Ni [9]. Second, the binding energy for both substitutional and interstitial He atoms approaches zero at a distance of about 0.7 nm from the GB. Similar results were obtained for the other GBs investigated in this study. This 'capture radius' depended on GB properties. The $\Sigma 3$ {1 1 2} GB, with the lowest GB energy and V_{gb}/A, gave a capture radius of only ~0.3 nm. Third, the He binding energy is highly non-uniform in the GB core. There appears to be a rough correspondence between the distance dependence of the He

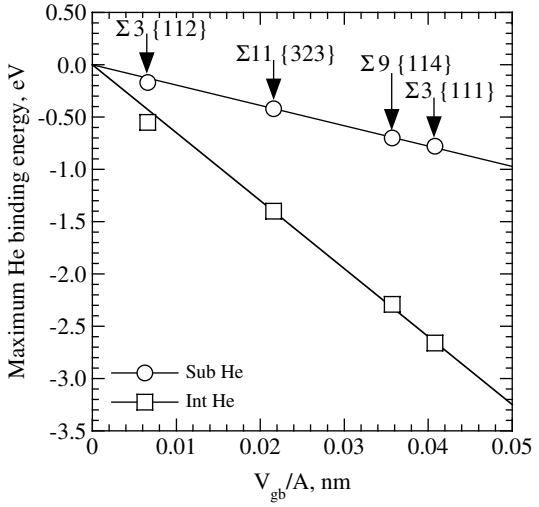

Fig. 4. Dependence of the maximum He binding energy on GB excess volume.

binding energies and the excess volume, but this is certainly not unequivocal. As shown in the plot in Fig. 4 there is an excellent correlation between the maximum binding energy for both substitutional and interstitial He and the GB excess volume.

4. Conclusions

Atomistic computer simulations were used to explore the effect of GB structure on the binding energy of He in Fe. Symmetrical tilt GBs spanning a range of GB energies and excess volumes were examined. While symmetrical tilt GBs represent only a small fraction of the GB character distribution in actual materials, the present results span a wide range of GB properties, and therefore are likely relevant to more complex GB structures. The results demonstrated that both substitutional and interstitial He atoms were bound to all of the GBs studied. Interstitial He was more strongly bound ($E^i_{gb} \sim 0.5$–2.7 eV) to the GB core than substitutional He ($E^s_{gb} \sim 0.2$–0.8 eV). The binding energy of He was found to increase linearly with GB excess volume. The capture radius for a He atom varied from ~0.3 to 0.7 nm and also depended on GB properties. Lastly, the He binding energy varied significantly within the GB core and approximately corresponded to the variation in atomic excess volume normal to the GB plane. Further work is needed to investigate the effect of multiple He atoms and vacancies on binding to GBs. In addition, migration of He along the GB is an important transport mechanism that will be the subject of a future atomistic study.

Acknowledgements

This research was supported by the US Department of Energy, Office of Fusion Energy Sciences, under contract DE-AC06-76RLO1830.

References

[1] H. Ullmaier, Nucl. Fus. 24 (1984) 1039.
[2] A. Ryazanov, D.N. Braski, H. Schroeder, H. Trinkaus, H. Ullmaier, J. Nucl. Mater. 233–237 (1996) 1076.
[3] A. Ryazanov, R.E. Voskoboinikov, H. Trinkaus, J. Nucl. Mater. 233–237 (1996) 1085.
[4] R.L. Klueh, D.J. Alexander, J. Nucl. Mater. 218 (1995) 151.
[5] M.I. Baskes, MRS Bull. (1986) 14.
[6] M.I. Baskes, M.S. Daw, in: N.R. Moody, A.W. Thompson (Eds.), Hydrogen Effects on Material Behavior, TMS, Warrendale, PA, 1990, p. 717.
[7] K. Farrell, P.J. Maziasz, E.H. Lee, L.K. Mansur in: H. Ullmaier (Ed.), Fundamental Aspects of Helium in Metals, Radiat. Eff. 78 (1983) 1.

[8] W.D. Wilson, C.L. Bisson, M.I. Baskes, Phys. Rev. B 24 (1981) 5616.
[9] M.I. Baskes, V. Vitek, Met. Trans. A 16 (1985) 1625.
[10] J.H. Evans, A. van Veen, J.T.M. de Hosson, R. Bullough, J.R. Willis, J. Nucl. Mater. 125 (1984) 298.
[11] J.T.M. de Hosson, J.R. Heringa, S.W. Schapink, J.H. Evans, A. van Veen, Surf. Sci. 144 (1984).
[12] W.D. Wilson, M.I. Baskes, M.S. Daw, in: R.M. Latanision, T.E. Fisher (Eds.), Advances in the Mechanics and Physics of Surfaces, Harwood Academic, 1983, p. 1.
[13] M.I. Baskes, C.F. Melius, W.D. Wilson, in: J.K. Lee (Ed.), Interatomic Potentials and Crystalline Defects, TMS, Warrendale, PA, 1981, p. 249.
[14] J.T.M. de Hosson, A.W. Sleeswyk, L.M. Caspers, W. van Heugten, A. van Veen, Solid State Commun. 18 (1976) 479.
[15] F. van d. Berg, W. van Heugten, L.M. Caspers, A. van Veen, J.T.M. de Hosson, Solid State Commun. 24 (1977) 193.
[16] J.B. Adams, W.G. Wolfer, J. Nucl. Mater. 158 (1988) 25.
[17] H. Trinkaus, B.N. Singh, M. Victoria, J. Nucl. Mater. 233–237 (1996) 1089.
[18] J.H. Evans, A. van Veen, J. Nucl. Mater. 233–237 (1996) 1179.
[19] H. Shiraishi, J. Nucl. Mater. 233–237 (1996) 985.
[20] V.M. Chernov, V.A. Romanov, A.O. Krutskikh, J. Nucl. Mater. 271&272 (1999) 274.
[21] K. Morishita, R. Sugano, B.D. Wirth, T. Diaz de la Rubia, Nucl. Instrum. and Meth. B 202 (2003) 76.
[22] R.J. Kurtz, R.G. Hoagland, J.P. Hirth, Philos. Mag. A 79 (1999) 665.
[23] R.J. Kurtz, R.G. Hoagland, J.P. Hirth, Philos. Mag. A 79 (1999) 683.
[24] V. Vitek, A.P. Sutton, D.A. Smith, R.C. Pond, in: Grain Boundary Structure and Kinetics, American Society for Metals, Metals Park, OH, 1980, p. 115.
[25] H. Grimmer, W. Bollman, D.H. Warrington, Acta Cryst. A 30 (1974) 197.